Journal of the European Ceramic Society **16** (1996) 1149–1156

PII:S0955-2219(96)00052-0
0955-2219/96/$15.00

Protonic Conduction in $Sr_{1-y}(Zr_{1-x}Dy_x)O_{3-\delta}$ Ceramics

B. Gharbage,[a] F. M. B. Marques[b,*] & J. R. Frade[b]

[a]Instituto Politécnico de Viana do Castelo, ESTG, Ap. 51, 4900 Viana do Castelo, Portugal
[b]Departamento de Engenharia Cerâmica e do Vidro, Universidade de Aveiro, 3810 Aveiro, Portugal

(Received 30 November 1995; revised version received 12 February 1996; accepted 20 February 1996)

Abstract

Ceramic materials derived from strontium zirconate were prepared by high-temperature solid-state reaction starting from oxides and carbonates. Distorted ABO_3-type perovskite structures, indexed to the orthorhombic system, were obtained for A-site substoichiometric and/or B-site Dy-doped materials. The conductivity of $Sr(Zr_{1-x}Dy_x)O_{3-\delta}$ is slightly lower than found for Y-doped strontium zirconate with identical trivalent dopant content, and increases with water vapour pressure, as expected for proton-conducting materials. For Dy-free perovskites with slight A-site substoichiometry ($Sr_{1-y}ZrO_{3-\delta}$, with $y \leq 0{\cdot}02$), the conductivity drops a few orders of magnitude and is nearly independent of water vapour pressure. The corresponding B-site doped materials [$Sr_{1-y}(Zr_{1-x}Dy_x)O_{3-\delta}$] have the highest conductivities, again dependent on water vapour pressure. This indicates that B-site doping is essential to obtain significant proton conductivity. The behaviour of these materials can be understood based on a classical defect chemistry type of approach, if one assumes that electron hole mobilities at low temperature ($\approx 300°C$) are smaller than for protons. This trend is reversed at higher temperatures ($>500°C$). For highly substoichiometric perovskites ($y \geq 0{\cdot}05$), even when B-site doped, the conductivity is minimal and independent of water vapour pressure. A blocking intergrain phase is believed to control the electrical transport properties of these materials. Copyright © 1996 Elsevier Science Ltd

1 Introduction

Protonic conduction has been found in several ABO_3 perovskite materials derived from strontium or barium cerates and zirconates, with B-site doping by Y, Yb, Nd, etc.[1–8] The basis for interpreting the behaviour of these materials was formulated by the pioneering work of Iwahara and co-authors,[1,2] who explained the observed dependence of electrical conductivity on water vapour pressure (P_w) by the formation of mobile protonic defects. Proton conductivity increases with P_w in cerates and zirconates,[2,5–7] even at relatively low temperatures when grain boundaries might play a significant role on the behaviour of polycrystalline ceramics. Nevertheless, results obtained with single crystals of Y-doped $SrZrO_3$ showed that bulk conductivity is also higher in wet than in dry atmospheres, and this demonstrates that protonic conduction is clearly a bulk property.[6]

Most cerate and zirconate materials have been studied at temperatures higher than about 600°C. However, lower temperature applications might also be feasible. For example, Iwahara *et al.*[8] used $BaCe_{0.9}Nd_{0.1}O_{3-\delta}$ as efficient H_2 sensors for temperatures down to about 200°C. Results reported by Liu and Nowick[5] showed that Nd-doped $BaCeO_3$ materials might also be used for water vapour sensors at temperatures of about 450°C. This suggests that further attention should be paid to the low-temperature behaviour of these materials.

Dy instead of Y is an obvious option for B-site doping, considering the similarities between the corresponding cations. In the case of $BaZrO_3$, it has been found that maximum conductivities are observed for Y or Dy B-site doped materials.[9] The information available on Dy-doped $CaZrO_3$ is that the sinterability is poor, but no reference has been found on the role of this dopant in $SrZrO_3$.[9] Also, A-site substoichiometry is expected to cause changes in transport properties as found for $LaMnO_3$-based materials,[10] and might also explain the improved electrical conductivity and sinterability of $SrZrTi_xO_{3+\delta}$ relative to $SrZrO_3$.[11] Metal vacancies can be compensated by different positive defects depending on working conditions. Improved densification might also be expected for A-site

*To whom correspondence should be addressed.

substoichiometric perovskites, when metal vacancies are relevant for the sintering process as found in many circumstances. The purpose of this work was thus to investigate the low-temperature behaviour of some $SrZrO_3$-based materials, using substoichiometry in the perovskite A-site position to test both the effectiveness of metal vacancies in originating protonic defects for charge compensation, and the role of this parameter on the sinterability of Dy-doped ceramics.

2 Experimental Procedure

Dy-doped strontium zirconate specimens of generic formula $Sr_{1-y}(Zr_{1-x}Dy_x)O_{3-\delta}$, with $y \leq 0{\cdot}10$ and $x \leq 0{\cdot}10$, were synthesized by solid-state reaction of oxides and carbonates. The compositions being studied include A-site stoichiometric and B-site doped materials of generic formula $[Sr(Zr_{1-x}Dy_x)O_{3-\delta}]$, A-site substoichiometric and B-site undoped zirconates $[Sr_{1-y}ZrO_{3-\delta}]$ and both A-site deficient and B-site doped materials $[Sr_{1-y}(Zr_{1-x}Dy_x)O_{3-\delta}]$. ZrO_2, Dy_2O_3 and $SrCO_3$ were mixed in a ball mill, calcined at 1350°C, pressed isostatically and sintered at 1650–1700°C for 2 h. Each material was characterized by scanning electron microscopy (SEM) and X-ray diffraction (XRD).

The electrical behaviour was investigated by impedance spectroscopy on discs with about 15 mm diameter and 2 mm thickness, using an HP4284A FRA in the 20–10^6 Hz frequency range. Measurements were undertaken at temperatures in the range 290–840°C, with partial pressures of water vapour in the range 3×10^2 to 8×10^3 Pa, using air or N_2 as carrier gas. The water vapour dosage in the gas phase was obtained by saturation of the carrier gas at different temperatures, or using a desiccant (sulfuric acid). Measurements were recorded after reaching steady state, which required less than 1 h.

3 Results and Discussion

3.1 Structure and microstructure

X-Ray diffractograms showed distorted perovskite structures, which were indexed to the orthorhombic system. Strontium deficiency and increasing Dy content caused a decrease in unit cell parameters. Furthermore, the diffractograms of samples with strontium deficiency >5% showed an extra peak attributed to cubic zirconia. The intensity of this peak increased with rising substoichiometry. In addition, SEM micrographs combined with energy-dispersive spectroscopy (EDS) showed

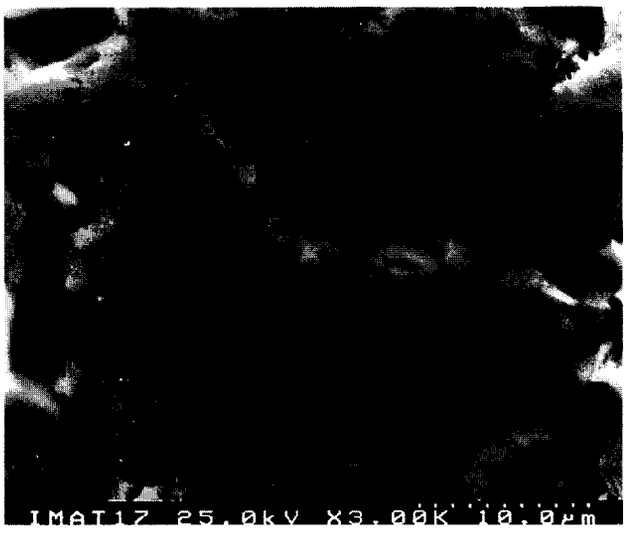

(a)

(b)

Fig. 1. Microstructure of a Sr deficient composition: (a) fracture surface showing vestiges of a liquid phase in between grains; (b) after polishing and thermal etching, showing the presence of a second phase mostly concentrated in triple contact points between grains.

a Zr- and Dy-rich amorphous phase located at grain boundaries [Fig. 1(a)]. During thermal etching it is believed that this phase concentrates mostly in triple contact points between grains [Fig. 1(b)]. Density measurements and SEM observations of this and the remaining compositions revealed significant porosity and poor microstructures in most specimens. The densities of A-site substoichiometric materials were about 90% of theoretical density, and the densities of corresponding A-site stoichiometric materials were slightly lower (between 80 and 90%). This means that, in general, substoichiometry indeed gave rise to improved densities.

3.2 Conductivity dependence on water vapour pressure, in air

Figure 2 shows typical impedance diagrams for $Sr(Zr_{0{\cdot}9}Dy_{0{\cdot}1})O_{3-\delta}$ at 400°C, in wet air with different

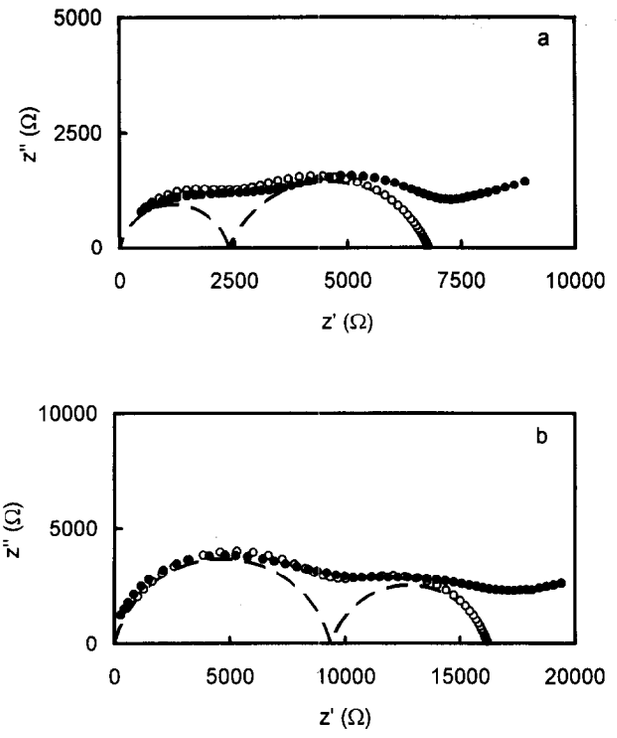

Fig. 2. Impedance diagrams for $Sr(Zr_{0.9}Dy_{0.1})O_{3-\delta}$ at 400°C, in wet air with different water contents: (a) P_w=7·3 × 10^3 Pa; (b) P_w=3 × 10^2 Pa. Solid lines correspond to estimated bulk and grain boundary contributions while the resulting total impedance is shown as open symbols.

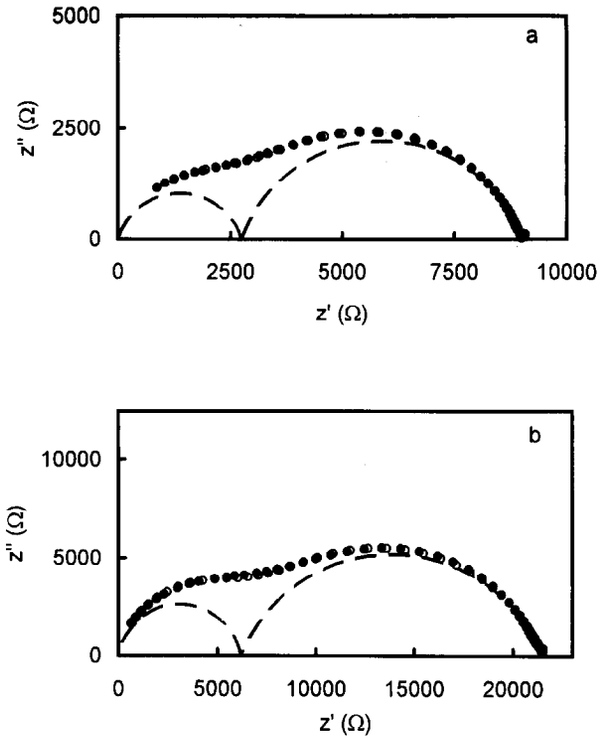

Fig. 3. Impedance diagrams for $Sr_{0.98}(Zr_{0.9}Dy_{0.1})O_{3-\delta}$ at 290°C, in wet air with different water contents: (a) P_w=7·3 × 10^3 Pa; (b) P_w=3 × 10^2 Pa. Solid lines correspond to estimated bulk and grain boundary contributions while the resulting total impedance is shown as open symbols.

water contents (P_w = 7·3 × 10^3 and 3 × 10^2 Pa). Arcs tend to be depressed but this might be related to poor densification of these materials, rather than to the intrinsic electrical behaviour of this composition. In fact, several samples of different microstructures are often needed to assess the effects of porosity and densification on impedance spectra.[12] However, this was not the objective of the present work, and the following discussion will be based on the experimental finding that the spectra can be solved simply into two arcs. The high-frequency arc goes through the origin and will be assigned to the bulk behaviour, while the second arc in the medium frequency range will be attributed to blocking effects due to grain boundaries. These bulk and grain boundary arcs are sensitive to humidity, which demonstrates the existence of protonic conductivity. In addition, the interfacial impedance at low frequencies is also dependent on water vapour pressure, which suggests that the main charge carriers are ionic, at least at low temperature.

Figure 3 shows the diagrams for $Sr_{0.98}(Zr_{0.9}Dy_{0.1})O_{3-\delta}$ at 290°C, in wet air with different water contents. Again, the bulk and grain boundary arcs are sensitive to humidity, which demonstrates the existence of a protonic conductivity contribution. This composition has the highest conductivity, and was thus selected for the remaining part of this study.

Figure 4 shows that the impedance spectrum obtained for $Sr_{0.98}ZrO_{3-\delta}$ at 600°C, in wet air (P_w = 2 × 10^3 Pa), reduces to a single arc; this can probably be attributed to the resistive grain boundary. In fact, expanding the high-frequency data reveals a small contribution, which remained unnoticed on using a much larger scale required for representing the grain boundary contribution. Total impedance is nearly independent of humidity, which indicates that protonic conductivity is negligible. In addition, comparison of data shown in Figs 2–4, and consideration of the differences in temperature, also show that the overall impedance of $Sr_{0.98}ZrO_{3-\delta}$ is much higher than for the remaining compositions with small or no A-site substoichiometry, and B-site doped [$Sr_{1-y}(Zr,Dy)O_{3-\delta}$, $y \leq 0.02$].

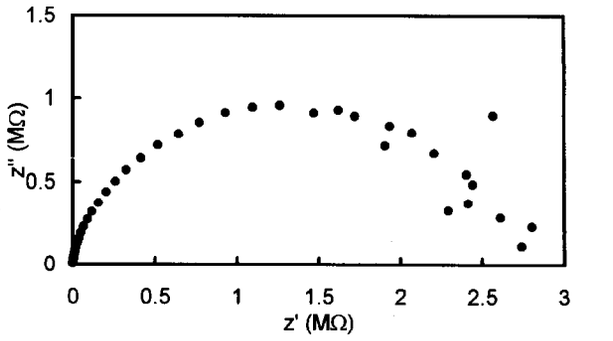

Fig. 4. Impedance diagram for $Sr_{0.98}ZrO_{3-\delta}$ at 600°C, in wet air (P_w=2 × 10^3 Pa). No significant difference was found on changing the water vapour pressure.

3.3 Dependence of conductivity on composition and temperature

The role of composition in the electrical behaviour can be further demonstrated by the temperature dependence of conductivity shown in Fig. 5 for several samples in wet air. $Sr_{0.95}(Zr_{0.95}Dy_{0.05})O_{3-\delta}$ (curve d) is highly resistive when compared with the other compositions. The liquid phase located at grain boundaries of this highly substoichiometric composition might be responsible for the resistive effect (see again Fig. 1). An intermediate level of conductivity is observed for the Dy-free composition (curve c). The activation energies found for these highly resistive compositions were about 1·8 and 1·5 eV, respectively. These high activation energies also indicate that protonic conductivity is not dominant in these materials.

A third level of conductivity is observed for Dy-doped materials with relatively small or no substoichiometry in the A-site (curves a and b). The conductivities of these compositions are somewhat smaller than for Y-doped $SrZrO_3$, and the activation energies (0·7–0·8 eV) are slightly higher than those reported for other proton-conducting perovskite materials.[13,14] However, this does not exclude protonic conduction because the overall behaviour is probably strongly influenced by grain boundary effects. For example, the temperature dependence of bulk and grain boundary conductivities of $Sr_{0.98}(Zr_{0.90}Dy_{0.10})O_{3-\delta}$ corresponds to activation energies of 0·54 and 0·78 eV, respectively. Note that the value for the activation energy of bulk conductivity is in close agreement with values reported for Y-doped $SrZrO_3$ single crystals.[14]

A slight enhancement in conductivity can be seen for materials with a small A-site deficiency and 10% Dy (Fig. 5, curves a and b). Improved conductivity for A-site substoichiometric compositions might correspond only to improved densification of these samples. Data corresponding to curves a and c suggest that B-site doping is essential in determining protonic conductivity. Negative defects originated by A-site substoichiometry might also originate protonic defects for charge compensation, but this idea finds no support in the present experimental observations.

3.4 Effect of P_w and P_{O_2} on the conductivity of $Sr_{0.98}(Zr_{0.9}Dy_{0.1})O_{3-\delta}$

Figures 2 and 3 have already shown that water vapour pressure affects the electrical conductivity of different samples. A more detailed study was carried out for the composition with the highest conductivity. The effect of water vapour pressure on the conductivity of $Sr_{0.98}(Zr_{0.9}Dy_{0.1})O_{3-\delta}$ when air and nitrogen are used as carrier gases is shown in Fig. 6.

The nitrogen used in these experiments has a small oxygen content, corresponding to an oxygen partial pressure (P_{O_2}) of the order of 1–10 Pa, which is three to four orders of magnitude smaller than in air (21 kPa).

A dependence of conductivity on $P_W^{1/2}$ is observed in air, at low temperatures (290°C), and for P_w lower than about 2×10^3 Pa. Impedance spectra used to separate the bulk from grain boundary contributions have demonstrated that bulk and grain boundary conductivities both increase approximately with $P_W^{1/2}$, at least within a limited range of working conditions. This conductivity dependence on water vapour pressure is in general agreement with the predicted behaviour for these protonic conductors and has already been reported for other protonic conductors.[2] The negligible dependence of conductivity on water

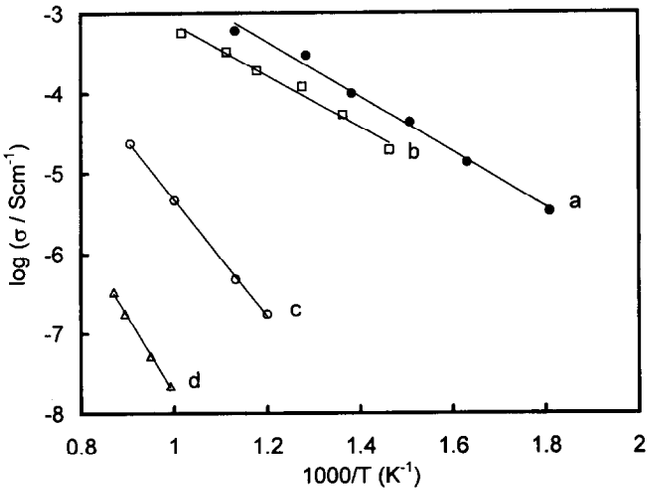

Fig. 5. Arrhenius plot of total conductivity for several samples in wet air (P_w ranging from 3×10^3 to 4×10^4 Pa): (a) $Sr_{0.98}(Zr_{0.9}Dy_{0.1})O_{3-\delta}$; (b) $Sr(Zr_{0.9}DY_{0.1})O_{3-\delta}$; (c) $Sr_{0.98}ZrO_{3-\delta}$; (d) $Sr_{0.95}(Zr_{0.95}Dy_{0.05})O_{3-\delta}$.

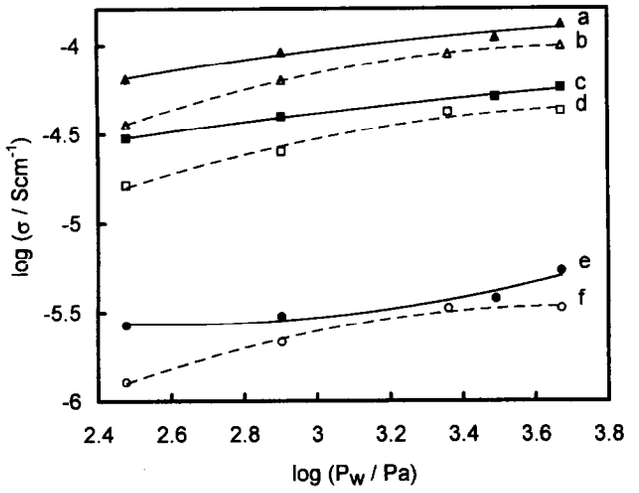

Fig. 6. Effect of P_w on conductivity of $Sr_{0.98}(Zr_{0.9}Dy_{0.1})O_{3-\delta}$ when N_2 (solid lines) or air (dashed lines) is used as carrier gas. Curves (a), (b) 450°C; (c), (d) 400°C; (e), (f) 290°C.

vapour pressure above certain values can be understood as a saturation effect, which ideally should correspond to full charge compensation of the dopant by protons.[5]

From curves shown in Fig. 6 a few more general observations can be made: (1) at constant temperature the conductivity is higher when nitrogen is used as a carrier gas than in air with identical moisture content; (2) the difference in conductivity in air and nitrogen is higher the lower the water vapour partial pressure; and (3) conductivity always increases with increasing water vapour pressure. These data were found to be reproducible in different runs. The differences shown in Fig. 6 cannot be attributed to electron hole conductivity which should be small in all cases at temperatures much lower than 600°C.[7] Also, hole conductivity is usually expected to increase with increasing oxygen partial pressure, and this is contradicted by experimental evidence. In fact, data previously published show that, at relatively high temperature, the electrical conductivity in dry atmospheres (oxygen, air and nitrogen) tends to increase with P_{O_2}.[1] This trend has also been observed in the present experiments at temperatures of the order of 800°C. A justification for this behaviour is attempted in the next section.

3.5 Defect chemistry of $SrZrO_3$-based protonic conductors

Using Kroger–Vink notation, the following equation suggested by Iwahara and co-workers[1,2] can be used to describe the formation of protonic defects in oxides:

$$H_2O\ (g) + 2h^{\cdot} = 2H_i^{\cdot} + 1/2\ O_2\ (g) \qquad (1)$$

To discuss in further detail the relations between composition, conductivity and working conditions (temperature, P_w and P_{O_2}), it is desirable to assume some type of dominant intrinsic ionic defects. In a previous paper we have shown that dominant Schottky-type defects can provide a good basis for interpretation of the transport properties of these materials.[15] This was also assumed in the present work when attempting to prepare A-site deficient perovskites. The dominant negative defects might be strontium vacancies (V_{Sr}'') or Dy ions in the B-site (Dy_{Zr}'), and their concentrations depend on the A-site substoichiometry and B-site dopant levels. The relevant positive defects involved in charge transport should be in this case oxygen vacancies ($V_O^{\cdot\cdot}$), electron holes ($h^{\cdot}$) and protons ($H_i^{\cdot}$). In addition, interaction between ionic and electronic defects can be obtained from usual defect formation reactions:

$$O_O = 1/2\ O_2\ (g) + V_O^{\cdot\cdot} + 2e' \qquad (2)$$

$$0 = V_{Sr}'' + V_{Zr}'''' + 3V_O^{\cdot\cdot} \qquad (3)$$

$$e_v = e' + h^{\cdot} \qquad (4)$$

Equations (2) and (4) can be combined to describe directly the interaction between instrinsic positive defects, which gives:

$$O_O + 2h^{\cdot} = 1/2\ O_2\ (g) + V_O^{\cdot\cdot} \qquad (2a)$$

Reactions (2)–(4) describe the formation of oxygen vacancies, Schottky defects and electronic defects, respectively, and the corresponding equilibrium constants can be written in the usual manner.

For a given composition one may compute $[V_{Sr}'']$ and $[Dy_{Zr}']$, but finding suitable relations between defect concentrations and water vapour or oxygen partial pressures still requires additional relations. The first one is derived from the unit A:B site ratio in the perovskite, including cation vacancies and Dy for Zr substitution:

$$[Sr_{Sr}] + [V_{Sr}''] = [Zr_{Zr}] + [Dy_{Zr}'] + [V_{Zr}''''] \qquad (5)$$

A relation between P_w and P_{O_2} might also be needed in reducing conditions. In fact, reducing conditions are usually achieved with H_2-containing gas mixtures, on assuming equilibrium between H_2, O_2 and H_2O. Similarly, water vapour might be reduced to H_2 by electrochemical pumping, and combination with a mass balance of hydrogen yields P_w as a function of P_{O_2}. All defect concentrations can thus be related to P_{O_2}.[13] Nevertheless, the H_2:H_2O ratio becomes negligible in relatively oxidizing conditions, and in this case P_w and P_{O_2} can be adjusted independently. This condition holds for the experimental conditions selected for this work.

The third relation required to evaluate the effects of water vapour and oxygen partial pressures on the concentration of charge carriers is obtained on assuming electroneutrality for the combined contributions of all charged defects. However, a simple procedure for obtaining solutions is usually based on selecting pairs of one negative defect and one positive defect, each pair being dominant within a certain range of working conditions. A set of consecutive simplified electroneutrality conditions are thus obtained on changing P_{O_2} or P_w; this is certainly valid when the material's behaviour can be studied within large ranges of working conditions and dominant defects can be clearly identified. However, this is not possible when the range of values of P_{O_2} or P_w is relatively small, as for the present work, and it has been considered useful to work with a more general electroneutrality condition, based on one single negative defect and three positive defects. The rationale for this will become obvious from the following discussion.

The work being reported now has involved mostly perovskites with a slight deficit at the A-site and a relatively high dopant concentration at the B-site. For this reason it can be assumed that Dy'_{Zr} dominates over the remaining negative defects. Also, it has been shown that proton conduction is not expected when substoichiometry dominates the formation of negative-charged defects in these materials, which means that A-site substoichiometry must be much smaller than the trivalent dopant content for significant protonic conductivity to be retained. This is a further reason to concentrate our attention on negative defects originated by B-site doping. On the other hand, the dominant positive defects ($h^{\cdot}$, $V_o^{\cdot\cdot}$ or $H_i^{\cdot}$) might change depending on working conditions, and a partly simplified electroneutrality condition can be written as:

$$[Dy'_{Zr}] = p + 2[V_o^{\cdot\cdot}] + [H_i^{\cdot}] \qquad (6)$$

This is the same as neglecting the role of A-site vacancies, including those formed by Schottky disorder [reaction (3)].

The method for obtaining solutions for the defect diagram can now be based on using the equilibrium constant K_1 of reaction (1) to express p as a function of P_w, P_{O_2} and $[H_i^{\cdot}]$, and then using this result and equilibrium constants K_2 and K_4 of reactions (2) and (4) to express $[V_o^{\cdot\cdot}]$. Substitution of both expressions in eqn (6) thus yields

$$[H_i^{\cdot}] = [-\beta + (\beta^2 - 4\,\alpha\gamma)^{1/2}]/2\alpha \qquad (8)$$

with $\alpha = (1 + P_{O_2}^{1/4}/(K_1P_w)^{1/2})$, $\beta = (2K_2/K_4^2K_1P_w)$ and $\gamma = -[Dy'_{Zr}]$. Note that it has been assumed here that P_{O_2} and P_w can be adjusted independently, as expected for oxidizing conditions. For a specific set of values for equilibrium constants K_i, and partial pressures P_{O_2} and P_w, one computes the value of proton concentration, and the remaining defect concentrations can be easily calculated from that value.

This method can be used to predict defect diagrams for variable P_w while keeping P_{O_2} constant, or vice-versa. For example, Fig. 7 was obtained following this approach. Solid lines are for air P_{O_2} = 21 kPa), and the dashed lines are for a typical condition expected for commercial N_2 ($P_{O_2} \approx 10$ Pa). The values for the K_i were adjusted to ensure that working conditions identical to those used in this work would be consistent with the experimental trends already reported, namely that a dominant protonic conductor would have increasing conductivity on increasing the water vapour partial pressure at constant P_{O_2}, and higher conductivity in N_2 than in air, at constant P_w. The partial defect diagrams shown in these figures indeed indicate that such behaviour is possible if protons

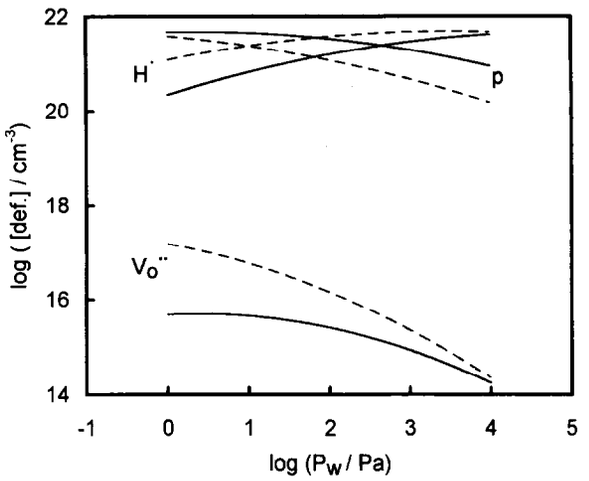

Fig. 7. Suggested defect diagram for Dy-doped $SrZrO_3$-based ceramics, at constant oxygen partial pressure and variable water vapour pressure. Solid lines: P_{O_2} = 21 kPa; dashed lines: P_{O_2} = 10 Pa.

and electron holes are the dominant positive defects, but only if the mobility of protons is higher than hole mobility in this range of temperatures. If this assumption is true, Fig. 8 also suggests that differences in conductivity between experiments performed in air and nitrogen must decrease with increasing water vapour pressure. In fact, this agrees with the experimental trend found at relatively low temperatures (see Fig. 6). While the trends of defect concentrations are commonly accepted in most of the work previously reported on this type of proton-conducting material, the suggested relationship between defect mobilities is not obvious and requires further discussion.

3.6 Final remarks

A comprehensive explanation of experimental data now being reported would require proton

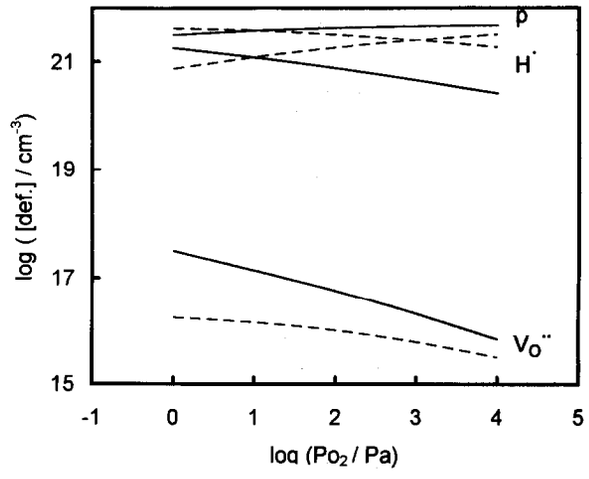

Fig. 8. Suggested defect diagram for Dy-doped $SrZrO_3$-based ceramics, at constant water vapour pressure and variable oxygen partial pressure. Solid lines: P_w = 1 Pa; dashed lines: P_w = 100 Pa.

and hole concentrations of the same order of magnitude, and dominant proton conductivity. This can only be achieved with an electron hole mobility lower than proton mobility in the temperature range 300–500°C. Measurements on proton concentration and mobility have already been reported in the literature and indicate that the concentration of protons is usually insufficient to balance the negative charges originated by B-site doping.[5] This means that most of the simplified electroneutrality conditions indeed include either a contribution by oxygen vacancies, a contribution by electron holes, or both. Expected mobilities of protons can also be found in the literature,[4,16] with activation energies in the range 0·5–0·6 eV, and extrapolation to lower temperatures yields values of about 9×10^{-8} and 5×10^{-7} cm^2 V^{-1} s^{-1} for the mobility of protons in $SrCe_{0.95}Yb_{0.05}O_{3-\delta}$ at 300 and 500°C. The mobility of oxygen vacancies is expected to be quite low at temperatures lower than 500°C, and this excludes a significant oxygen-ion conductivity contribution at such low temperatures, even if the oxide vacancy concentration is significant. Finally, electron hole conduction is likely to occur, especially at relatively high temperatures. Most authors have found significant electron hole conductivity contribution at temperatures higher than about 600°C, and in air, but this should disappear at lower temperatures as a result of decreasing defect concentration and/or defect mobility.

To our knowledge electron hole mobilities have not been reported for these perovskite-type materials. Nevertheless, data reported for other materials might be useful to predict the order of magnitude for electron hole mobilities in $SrZrO_3$-based materials. In fact, this material can be viewed as an ordered structure in the system SrO–ZrO_2, and one might thus estimate the order of magnitude of electron hole mobilities from data reported for zirconia-based electrolyte materials.[17] Extrapolation from high temperatures with an activation energy of about 1·4 eV yields electron hole mobilities of about 1.7×10^{-10} and 1.9×10^{-7} cm^2 V^{-1} s^{-1} at 300 and 500°C. These values are lower than the above-mentioned predictions for proton mobilities, which shows that the possibility of predominant protonic conduction with major electron hole concentrations should not be ruled out at low temperature. This trend can be reversed at high temperatures because the activation energies for the mobility of protons are probably much lower than for the mobility of electron holes. Note also that, from reported data,[17,18] the relative magnitude of mobilities of electronic and ionic defects in YSZ is expected to be reversed with change in temperature.

The overall role of substoichiometry and Schottky-type disorder on the defect chemistry and electrical transport properties has so far been ignored in this discussion, for the sake of simplicity. However, an additional comment should be added for cases when the Dy^{3+} content is similar to or lower than the A-site substoichiometry. Dy^{3+} is a large cation which might replace both Sr^{2+} in A-site and Zr^{4+} in B-site positions in these perovskites. This means that writing formulae for these perovskites suggesting that all Dy is in the B-site position might be inaccurate. Indeed, if Dy^{3+} cations share both sites in the lattice, this would originate both positive and negative defects ($Dy_{Sr}^{\cdot}$ and Dy_{Zr}'), and a decrease in the overall concentration of effective charge carriers ($h^{\cdot}$, $H_i^{\cdot}$ or $V_O^{\cdot\cdot}$). However, this would have no major impact on the previous discussion which was based on the case when the content of Dy^{3+} is much higher than the A-site substoichiometry.

At last, a final comment on the possible existence of B-site substoichiometry. No attempt has been made to prepare such compositions. However, if the structure might accept a significant concentration of B-site vacancies, the overall result would still fit in the model behaviour previously described. The dominant negative defects, whether dopant cations or vacancies in the B-site, would have to be compensated by the same positive defects, and their relevance would depend on working conditions.

4 Conclusions

The low-temperature behaviour of a number of $SrZrO_3$-based ceramics without or with slight A-site substoichiometry, and B-site doping by Dy, is strongly influenced by resistive grain boundaries. This is clearly the result of the processing route, namely poor sinterability, which in general can be improved with a slight deficit in the perovskite A-site position. Nevertheless, A-site substoichiometry has been found to be useless in determining protonic conduction, while B-site doping has been found to be a fundamental requirement for significant proton conductivity. Water vapour affects both bulk and grain boundary conductivities, and the relevant dependence suggests that $Sr_{0.98}(Zr_{0.9}Dy_{0.1})O_{3-\delta}$ is a mixed proton and electron hole conductor. The relative importance of both conductivity components depends on temperature, water vapour and oxygen partial pressures. The role of oxygen partial pressure in the total conductivity can only be understood on assuming that electron holes at low temperature have mobilities lower than protons.

Acknowledgement

This work was sponsored by JNICT, Portugal, contract STRD/CTM/664/92.

References

1. Iwahara, H., Esaka, T., Uchida, H. & Maeda, N., *Solid State Ionics*, **3/4** (1981) 359.
2. Uchida, H., Maeda, N. & Iwahara, H., *Solid State Ionics*, **11** (1983) 103.
3. Uchida, H., Yoshikawa, H. & Iwahara, H., *Solid State Ionics*, **34** (1989) 103.
4. Uchida, H., Yoshikawa, H. & Iwahara, H., *Solid State Ionics*, **35** (1989) 229.
5. Liu, J. F. & Nowick, A. S., *Solid State Ionics*, **50** (1992) 131.
6. Huang, H. H., Ishigame, M. & Shin, S., *Solid State Ionics*, **47** (1991) 251.
7. Yajima, T., Suzuki, H., Yogo, T. & Iwahara, H., *Solid State Ionics*, **51** (1992) 101.
8. Iwahara, H., Uchida, H., Ogoki, K. & Nagato, H., *J. Electrochem. Soc.*, **138** (1991) 296.
9. Iwahara, H., Yajima, T., Hibino, T., Ozaki, K. & Suzuki, H., *Solid State Ionics*, **61** (1993) 65.
10. Takeda, Y., Nakai, S., Kojima, T., Kanno, R., Imanishi, N., Shen, G. Q., Yamamoto, O., Mori, M., Asakawa, C. & Abe, T., *Mater. Res. Bull.*, **26** (1991) 153.
11. Zboroska, M., Grylicki, M. & Zborowski, J., *Ceramurgia Int.*, **6** (1980) 99.
12. Kleitz, M., Pescher, C. & Dessemond, L., in *Science and Technology of Zirconia V*, eds S. P. S. Badwal, M. J. Bannister & R. H. J. Hannink. Technomic Publishing Co., Inc., Basel, 1993, p. 593.
13. Shin, S., Huang, H. H., Ishigame, M. & Iwahara, H., *Solid State Ionics*, **40/41** (1990) 910.
14. Huang, H. H., Ishigame, M. & Shin, S., *Solid State Ionics*, 7 (1991) 255.
15. Labrincha, J. A., Frade, J. R. & Marques, F. M. B., *Solid State Ionics*, **61** (1993) 71.
16. Iwahara, H., in *Proton Conductors — Solids, Membranes and Gels — Materials and Devices*, ed. P. Colomban. Cambridge University Press, Cambridge, 1992, p. 122.
17. Weppner, W., *Z. Naturforsch.*, **A31** (1976) 1336.
18. Kleitz, M., Fernandez, E., Fouletier, J. & Fabry, P., *Advances in Ceramics, Vol. 3*, ed. A. H. Heuer & L. W. Hobbs. American Ceramic Society, Columbus, OH, 1981, p. 349.